

Jim

**United States
Department of
Agriculture**

**Natural Resources
Conservation
Service**

**11 Campus Boulevard
Suite 200
Newtown Square, PA 19073
Phone 610-557-4233; FAX 610-557-4136**

Subject: SOI -- Geophysical Assistance

Date: 29 May 2003

To: Stephen K. Chick
State Conservationist
USDA-Natural Resources Conservation Service
Federal Building, Room 152
100 Centennial Mall North
Lincoln, NE 68508-3866

Ref: Bureau of Indian Affairs Case # AAO-1066/WN/03 and AAO-1067/WN/03

Purpose:

Working with representatives of the Ponca Tribe and the Santee Sioux Nation, ground-penetrating radar (GPR) and electromagnetic induction (EMI) were used in field investigations to locate unmarked graves within two cemeteries and buried structural remnants of the former Ponca Agency. In addition, the use of GPR in areas of Valentine and Boel soils was assessed.

Participants:

Bob Bickerstaff, Santee Utilities, Santee Sioux Nation, Niobrara, NE
Jim Doolittle, Research Soil Scientist, USDA-NRCS-NSSC, Newtown Square, PA
Neil Dominy, Soil Scientist, USDA-NRCS, Stanton, NE
Sam Kitto, Environmental Specialist, Ponca Tribe of Nebraska, Niobrara, NE
Roger Hammer, Soil Scientist, USDA-NRCS, O'Neill, NE
Gary McCoy, Soil Scientist, USDA-NRCS, Stanton, NE
Alvin Twiss, Land Manager, Santee Sioux Nation, Niobrara, NE
William Zanner, Conservation and Survey Division, University of Nebraska, Lincoln, NE

Activities:

All field activities were completed on 5 to 9 May 2003.

Summary of Results:

1. GPR is an appropriate tool for soil investigations (upper 2 to 3 m) in areas of Valentine and Boel soils. However, small amounts of 2:1 expanding lattice clay in sandy soil significantly reduce penetration depths.
2. With minor exceptions, soils at the selected archaeological sites had properties that were unfavorable to GPR. The high clay content, large proportion of 2:1 expanding lattice clay minerals with high cation exchange capacities, and high carbonate contents of these soils produced highly conductive mediums. These mediums rapidly attenuate the radar signal and limit the depth of penetration and the detection of subsurface features. Because of high rates of signal attenuation, high levels of background noise plagued radar records and confounded interpretations.
3. GPR proved to be an unsatisfactory tool for burial detection. As confirmed in the radar record shown in Figure 6, in these soils, burials provide little enduring and unambiguous reflectors for GPR. If present, reflectors from burials are too small, faintly expressed, and indistinguishable from other features in the soil (burrows, roots, rock fragments). Processing of radar records provided some indication of the spatial distribution of subsurface anomalies, but could not unequivocally identify gravesites.

4. Within the suspected archaeological sites, buried features, if present, generally lacked sufficient size or contrast to be detected with EMI. Some anomalous EMI responses were measured at most sites. However, no clear and unambiguous EMI responses are available to support reliable gravesite interpretations.
5. All reported results are interpretative and based on the geophysical methods and the survey procedures used. As all archaeological sites represent sacred or sensitive areas, no ground-truth verification of interpretations was carried out during this investigation. Interpretations were therefore constrained.

It was my pleasure to work in Nebraska. The assistance of Gary McCoy and Roger Hammer was greatly appreciated.

With kind regards,

James A. Doolittle
Research Soil Scientist
National Soil Survey Center

cc:

- R. Ahrens, Director, USDA-USDA, National Soil Survey Center, Federal Building, Room 152, 100 Centennial Mall North, Lincoln, NE 68508-3866
- L. Hernandez, State Soil Scientist, USDA-NRCS, Federal Bldg., 100 Centennial Mall North, Lincoln, NE 68508-3866
- W. Maresch, Acting Director of Soils Survey Division, USDA-NRCS, Room 4250 South Building, 14th & Independence Ave. SW, Washington, DC 20250
- C. Murdy, Regional Archaeologist, USDI-BIA, Great Plains Regional Office, 115 Fourth Avenue SE, Aberdeen, SD 57401
- C. Olson, National Leader for Soil Investigations, USDA-USDA, National Soil Survey Center, Federal Building, Room 152, 100 Centennial Mall North, Lincoln, NE 68508-3866
- W. Tuttle, Soil Scientist (Geophysical), USDA-NRCS-NSSC, P.O. Box 974, Federal Building, Room 206, 207 West Main Street, Wilkesboro, NC 28697
- J. Wilmes, Resource Conservationists, USDA-NRCS, 111 North Washington Street, P.O. Box 300, Bloomfield, NE 68718-0300

Equipment:

The radar unit is the Subsurface Interface Radar (SIR) System-2000, manufactured by Geophysical Survey Systems, Inc.¹ Morey (1974), Doolittle (1987), and Daniels (1996) have discussed the use and operation of GPR. The SIR System-2000 consists of a digital control unit (DC-2000) with keypad, VGA video screen, and connector panel. A 12-volt battery powers the system. This unit is backpack portable and, with an antenna, requires two people to operate. Antennas with center frequencies of 200 and 400 MHz were used in this investigation.

The RADAN NT (version 2.0) software program developed by Geophysical Survey Systems, Inc., (2001a) was used to process the radar records.¹ Processing included color transformation, marker editing, distance and surface normalization, range gain adjustments, and migration. GPR data from the archaeological sites were processed into a three-dimensional image using the 3-D QuickDraw for RADAN Windows NT software developed by Geophysical Survey Systems, Inc. (2001b).¹ Once processed, arbitrary cross-sections and time slices were viewed and selected images saved to files.

The electromagnetic induction meter used in this study was the EM38DD, manufactured by Geonics Limited.¹ Geonics Limited (2000) describes the operating procedures of this meter. The EM38DD meter is portable and requires only one person to operate. No ground contact is required with this meter. The EM38DD operates at a frequency of 14,600 Hz. It has effective penetration depths of about 0.75 and 1.5 m in the horizontal and vertical dipole orientations, respectively. The EM38DD meter consists of two EM38 meters bolted together and electronically coupled. One meter acts as a master unit (meter that is positioned in the vertical dipole orientation and having both transmitter and receiver activated) and one meter acts as a slave unit (meter that is positioned in the horizontal dipole orientation with only the receiver switched on).

The Geonics DAS70 Data Acquisition System was used to record and store EMI data.¹ The acquisition system consists of an EM38DD meter and Allegro field computer. With this data acquisition system, the EM38DD meter is keypad operated and measurements can either be automatically or manually triggered.

To help summarize the results of this study, the SURFER for Windows (version 8) program, developed by Golden Software, Inc.,¹ was used to construct two-dimensional simulations. Grids were created using kriging methods with an octant search.

1. Soil Investigations:

Study Areas:

Two study sites were selected in western Knox County. Radar traverses and ground-truth core observations were collected at each site. The purpose of these investigations was to assess the potential of GPR in areas of coarse-textured soils formed in aeolian and alluvial deposits.

A radar traverse was conducted in an area that had been mapped as Valentine fine sand, 3 to 9 percent slopes (Schulte et al., 1997), in the southwest quarter of Section 15, T. 31 N., R. 7 W. The very deep, excessively drained Valentine soil formed in sandy eolian materials. Valentine is a member of the mixed, mesic Typic Ustipsamments family. The study site was located within a nature preserve. Relief was about 5.1-m along the GPR traverse line.

A radar traverse was also conducted across an area that had been mapped as Boel loamy fine sand, 0 to 2 percent slopes (Schulte et al., 1997), in the southeast quarter of Section 16, T. 33 N., R. 7 W. The very deep, somewhat poorly drained Boel soil formed in loamy and sandy alluvium on bottomlands. Boel is a member of the sandy, mixed, mesic Fluvaquentic Haplustolls family. The study site was in a field of alfalfa. Relief was not measured at this site.

Field Procedures:

A traverse line was established across each study site. At the Valentine soil site, the traverse was about 80-m long. At the Boel soil site, the traverse line was about 140-m long. Along each traverse line, survey flags were inserted in the ground at intervals of about 10-m (about 33 feet). The survey flags served as reference points. Pulling the 200 MHz antenna along each traverse line completed a radar survey file. As the radar antenna was pulled passed each flagged reference point, the operator impressed a vertical reference mark to identify the location of the point on the radar record.

¹ Trade names are used to provide specific information. Their mention does not constitute endorsement by USDA-NRCS.

At each site the depth to a known reflector was used to determine the velocity of propagation. The velocity of propagation and the dielectric permittivity is moisture dependent and varies with antenna frequency. At the time of this investigation, soils were moist in the upper part. For the upper part of the Valentine and Boel soils, with the 200 MHz antenna, the estimated velocity of propagation was about 0.08 m/ns and the dielectric permittivity was 14. These estimates were based on the depths (50 cm) to a buried metallic reflector.

Results:

Figure 1 is a radar record from the area of Valentine soil. The short, vertical lines at the top of the radar record represent equally spaced (10-m) reference points along the radar traverse. A vertical scale (in meters) appears along the left-hand margin of the record. Using measured elevation data, the radar record has been terrain corrected.

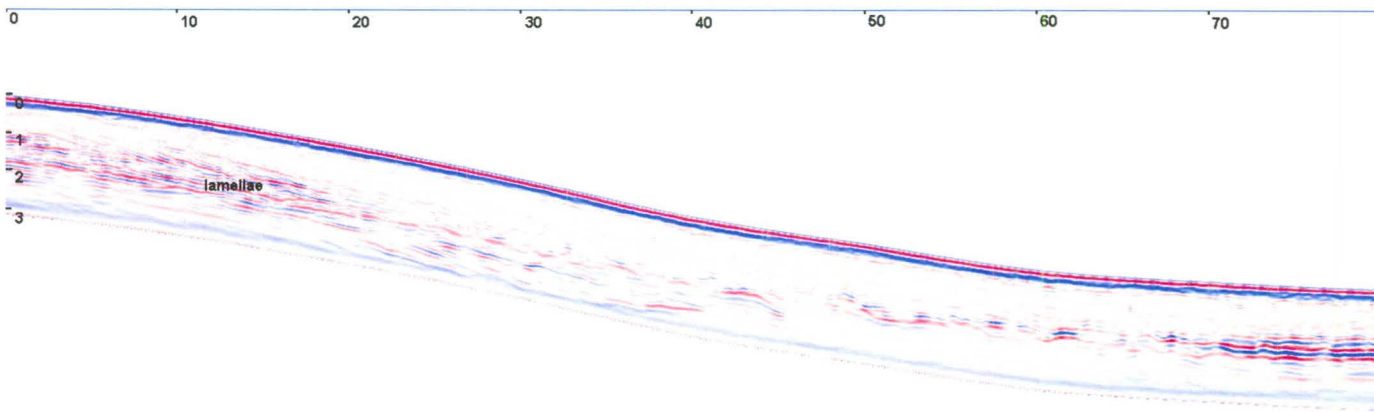


Figure 1. GPR record from an area of Valentine fine sand, 3 to 9 percent slopes.

Stratification and bands of lamellae are evident in this radar record (see Figure 1). Depth of penetration is slightly greater on the higher-lying portion of the traverse line. Here, multiple and often-intersecting linear reflectors are apparent. Assemblages or groups of similar radar reflection types (high-angle clinoforms, parallel/planar, sigmoidal, and hummocky/wavy) identify *radar facies* and record discrete intervals of deposition. Terminations of *radar facies* identify bounding surfaces that indicate erosional unconformities. High-angle clinoforms appear in the upper part of the soil profile on higher-lying, backslope positions and suggest slip-face accretion. Lower backslope positions are dominated by hummocky/wavy *radar facies* that suggest erosional or trough cross beds. Several high amplitude parallel/planar reflectors limit penetration to depths of less than 1.8 m on lower lying, swale position (right-hand portion of Figure 1). These reflectors consist of broader, more diffuse bands that suggest wetter and/or more attenuating soil properties. These reflectors represent buried surface layers or paleosols that have slightly higher clay (loamy fine sand and fine sandy loam textures) contents. The soil in this portion of the radar record is Doger. The very deep, well drained or somewhat excessively drained Doger soil formed in sandy materials on uplands. Doger is a member of the sandy, mixed, mesic Entic Haplustolls family.

With the 200 MHz antenna, the maximum depth of penetration in this area of Valentine soil was only about 2.8 m. This depth is surprisingly shallow for an excessively drained, sandy soil. Below this depth, radar reflections were exceedingly weak and indistinguishable from background noise. This rather rapid attenuation of electromagnetic energy is attributed to the clays that are found within thin bands of lamellae. A perplexing fact is that the clay content of these lamellae is very low, as the texture is typically loamy sand, and the lamellae are often thin and may be very few in numbers.

In Valentine soil, the fines are dominated by 2:1 expanding lattice clays. These clays (presumably smectitic) have a high cation exchange capacity (CEC), which causes the very rapid attenuation of the radar's electromagnetic energy. In very low clay content soils with clay minerals dominated by smectite, Olhoeft (1986) observed a rapid and significant increase

in the *loss tangent* (from 0.09 to 0.84) as the amount of smectite clays was increased from 0 to 4 percent by weight. The *loss tangent* ($\tan\delta = \sigma/\epsilon \cdot 2\pi$) is directly related to the conductivity (σ) and inversely related to the dielectric permittivity (ϵ) of the soil. The *loss tangent* is a measure of attenuation or dielectric adsorption. At 5 percent clay (by weight), the rise in *loss tangent* leveled off and remained constant at about 1.0 as the clay content was increased from 5 to 22 percent (maximum clay content used in Olhoeft's study). These findings of Olhoeft explain the rather restricted depths of penetration in Valentine soil, which has very small amounts of 2:1 lattice clays with high CECs.

Along the traverse line, soils were examined at two reference points. At one reference points, samples were obtained for characterization at the National Soil Laboratory. The sample site was on an upper back slope and in an area of Thurman soil. The very deep, somewhat excessively drained Thurman soil formed in sandy eolian material on uplands. Thurman is a member of sandy, mixed, mesic Udorthentic Haplustolls family.

Similar results were obtained in the area of Boel soil. Here strata of medium textured alluvial materials restricted penetration depths. Ground-penetrating radar effectively mapped the depth, form, and distribution of alluvial strata. *Radar facies* as well as bounding surfaces were evident on the radar record.

2. Archaeological Investigations

Overview:

Geophysical methods provide a rapid, nondestructive, and relatively low cost procedure for detecting soil disturbances and the intrusion of foreign materials. Geophysical methods are therefore useful in the search for buried archaeological features. Results vary with soil conditions. With minor exceptions, soils at the selected archaeological sites within Knox County had properties unfavorable to GPR. Most soils had high clay and carbonate contents, and were dominated by clay minerals with high cation exchange capacities. These factors caused the rapid attenuate of electromagnetic energy, which limited the radar's penetration depths and the resolution of subsurface features. In addition, buried cultural features, if present, lacked sufficient number, size, or contrast to be detected with EMI.

Even under more favorable site conditions the detection of burials can not be guaranteed with geophysical methods. The detection of burials is affected by (i) the electromagnetic gradient existing between a feature and the soil, (ii) the depth, size and shape of the buried feature, and (iii) the presence of scattering bodies within the soil (Vickers et al., 1976).

The amount of energy reflected back to an antenna or the electromagnetic response to a buried feature is a function of the electrical contrast existing between the medium and the buried feature. The greater and more abrupt the contrast in electrical properties, the greater the amount of energy reflected back to a radar antenna or the greater the contrast in the induce electromagnetic fields. Many recently buried features contrast with the surrounding soil matrix and signs of soil disturbance are often evident. However, with the passage of time, natural soil-forming processes erase the signs of disturbance, and buried features decay or weather and become less electrically contrasting with the surrounding soil matrix.

The size and depth of a buried feature affect detection. Large, contrasting objects are easier to detect than small non-contrasting objects. A shallowly buried feature is easier to detect that a deeply buried feature of similar size. In many soils, signal attenuation limits the observation depth of GPR. Because of its depth/response function, EMI is more sensitive to feature that occur at shallow depths. Compared with GPR, the resolution of EMI is coarser and small, less contrasting features are more likely to be overlooked.

Bones are difficult to detect with either method. Bevan (1991) noted that it is more likely that GPR will detect the disturbed soil within a grave shaft, a partially or totally intact coffin, or the chemically altered soil materials, which directly surrounds a burial, than the bones themselves. Killam (1990) observed that most bones are too small to be directly detected with GPR. This author noted that it is the disruption of soil horizons that makes most graves detectable with GPR.

Burials are difficult to distinguish with GPR in soils having numerous rock fragments, tree roots, animal burrows or stratified and segmented soil layers. These scattering bodies produce undesired subsurface reflections, which complicate radar records and mask the presence of burials. Under such conditions, burials are often indistinguishable from the background clutter.

Ponca Tribe of Nebraska

Study Areas:

GPR and EMI surveys were conducted in an area that was suspected to contain buried structural remnants of the former Ponca Agency near Ponca. The survey site is located in a grassed area that is bordered by a stream (to the east) in the southwest quarter of Section 25, T. 32 N., R. 7 W. The area had been mapped as Verdel silty clay, 0 to 2 percent slopes (Schulte et al., 1997). The very deep, well drained Verdel soil formed in clayey alluvium derived from Pierre shale on stream terraces. Verdel is a member of the fine, smectitic, mesic Vertic Haplustolls family. The solum of Verdel soil contains 35 to 60 percent clay. Free carbonates occur at depths of 20 to 30 inches.

GPR and EMI surveys were also conducted within St Johns Cemetery near Ponca. The purpose of this survey was to detect unmarked gravesites. This cemetery is also located in the southwest quarter of Section 25, T. 32 N., R. 7 W. The area had been mapped as Labu-Sansarc complex, 11 to 30 percent slopes; Labu silty clay, 6 to 11 percent slopes; and Simeon sand, 6 to 30 percent slopes, eroded (Schulte et al., 1997). The well drained, moderately deep Labu and shallow Sansarc soils formed in residuum weathered from clay shales. Typically the underlying soft clay shales are easily dug with a spade. The lower part of the C horizon and the underlying shale contain varying amounts of carbonates, gypsum and other salts. Soloms average between 45 and 70 percent clay. Labu is a member of the fine, smectitic, mesic Vertic Haplustepts family. Sansarc is a member of the clayey, smectitic, calcareous, mesic, shallow Typic Ustorthents family. The very deep, excessively drained Simeon soil formed in sandy alluvium on terraces. Simeon soil is a member of the mixed, mesic Typic Ustipsamments family.

Within St. Johns Cemetery, two sites were selected for detailed geophysical surveys. Both sites were located on slight knolls and each contained soils with noticeably coarser-textured surface layers (suggesting areas of Simeon soils). Site 1 was located along the southern boundary of the cemetery and to the immediate east of a clump of trees that contained several marked gravesites. Site 2 was located to the northeast of Site 1 and across the cemetery road. Site 2 was border on the north by a clump of trees and several marked gravesites. The western boundary of the grid was parallel with three headstones that were to the immediate north (about 1 m).

A suspected cemetery for victims of an early 1900 small pox epidemic was surveyed near the town of Santee. During an earlier excavation at this site, the bones of three individuals were exhumed. A perimeter fence was constructed around the site to protect other probable gravesites. A marker was erected within the site. The Santee Tribe wishes to confirm if other unmarked graves are located within this site. This suspected cemetery is located in the southeast quarter of Section 14, T. 33 N., R. 5 W. The site had been mapped as Verdigre loam, 6 to 11 percent slopes, and Redstoe silt loam, 6 to 11 percent slopes (Schulte et al., 1997). The deep, well drained Verdigre soil formed in loamy eolian material deposited over material weathered from clayey shales on uplands. Verdigre is a member of the fine-loamy, mixed, superactive, mesic Typic Argiustolls family. The moderately deep, well drained Redstoe soil formed in residuum weathered from chalky siltstone on uplands. Redstoe is a member of the fine-silty, mixed, superactive, mesic Typic Calciustolls family. Both Verdigre and Redstoe soils have textural control sections that contain between 18 and 35 percent clay and belong to the superactive cation exchange capacity class. These soils have layers of calcium carbonate enrichment.

With the exception of Simeon, all soils had properties unfavorable to GPR. The high clay content, large proportion of clay minerals with high cation exchange capacities, and high carbonate contents of these soils produced highly conductive mediums. These mediums rapidly attenuate the radar signal and limit the depth of penetration and the detection of subsurface features. In such high-loss mediums, the use of low frequency (<300 MHz) provides little improvement in penetration depths and significant reduction in the resolution of subsurface features. Sternberg and others (1995) noted that, in high-loss mediums, compared with lower frequency antennas (80 and 100 MHz), higher frequency antennas (500 MHz) provided much better resolution and similar depths of penetration. For this reason, only a 400 MHz antenna was used in the archaeological investigations.

Field Procedures:

Survey procedures were simplified to expedite the establishment of survey grids and fieldwork. At most sites, two parallel sets of lines were laid out. These lines helped to define the perimeter of a rectangular grid area. Dimensions of the grids were: 8 by 80 m (about 0.06 ha) at the suspected former Ponca Agency site, 10 by 15 m (0.015 ha) at the St Johns Cemetery sites, and 36 by 52 m (0.19 ha) at the suspected cemetery site near Santee (three parallel lines were used for this larger site). Along each line, survey flags were inserted in the ground at intervals of either 2 (Ponca Agency site) or 1 m. These flags served as grid line end points and provided ground control. Walking at a fairly uniform pace with either geophysical

device, between similarly numbered flags on opposing sets of parallel lines, in a back and forth pattern across each grid area completed both the GPR and EMI surveys.

Grid or traverse intervals of 1 or 2 m were used. These intervals are a compromise among the purpose of the survey, size of the area to be surveyed, features being identified, available time, desired detection probability, and desired position accuracy. Typically, intervals of 5 to 10 m have been used to define the general location of buried structures, and 1 to 3 m to locate buried hearths and foundation walls. To detect burials within designated or confined areas, grid or traverse intervals typically range from 15 to 150 cm (Bevan, 1991). Smaller intervals are required to detect these relatively small features. Even when closely spaced intervals (50 cm) and relatively high frequency antennas (>400 MHz) are used on favorable soils, burials can be overlooked and some subsurface features will be improperly interpreted as burials.

For each EMI survey, the EM38DD meter was operated in the continuous mode with measurements recorded at a 1-sec interval. The EM38DD meter was held about 1 to 2 inches above the ground surface with its long axis parallel to the direction of traverse. For each traverse line, the location of each measurement was later adjusted to provide a uniform interval between observation points.

Pulling the 400 MHz antenna along each grid line completed a radar survey file. To guide the GPR, a *measured* line was extended between similarly numbered flags on opposing end lines. Reference marks were spaced at either 1 or 2 (Santee site) m intervals along the *measured* lines. As the radar antenna was pulled passed each marked point on a *measured* line, the operator impressed a vertical reference mark on the radar record to identify the point.

Results:

EMI

Old Ponca Agency site:

Basic statistics for the data collected with the EM38DD meter at the Ponca Agency Site are shown in Table 1. Apparent conductivity increased and became more variable with increasing penetration depths. Apparent conductivity averaged 38.0 mS/m and 58.9 mS/m for measurements obtained in the shallower-sensing horizontal and deeper-sensing vertical dipole orientations, respectively. In the horizontal dipole orientation, apparent conductivity ranged from about 22 to 99.5 mS/m with a standard deviation of 11.1 mS/m. In the vertical dipole orientation, apparent conductivity ranged from about 31.5 to 102 mS/m with a standard deviation of 17.2 mS/m. Higher measurements reflect the interference from the metallic stock fence.

Table 1
Apparent conductivity data collected with the EM38DD meter at the Ponca Agency Site
All values are in mS/m.

	<u>Horizontal Dipole</u>	<u>Vertical Dipole</u>
Average	38.0	58.9
Standard Deviation	11.1	17.2
Minimum	22.0	31.5
Maximum	99.5	102.0
25% Quartile	30.4	46.1
75% Quartile	42.1	66.2

Figure 2 contains choropleth maps showing the spatial distribution of apparent conductivity collected with the EM38DD meter at the supposed site of the Ponca Agency. Each map was constructed from 495 observations. Color variations have been used to show the distribution of apparent conductivity. In each map, the color interval is 5 mS/m. In general, EMI responses were higher and more variable in the deeper-sensing (0 to 1.5 m), vertical dipole orientation (lower map) than in the shallower-sensing (0 to 0.75 m), horizontal dipole orientation (upper map). The survey area was bounded on the south and west by a metallic stock fence (the origin of the map is located about 5 and 12 feet from the fence lines that bound the survey area along its western and southern boundaries, respectively). These fence lines interfered with the meters' electromagnetic fields and produced the anomalously high responses along the bottom and lower left-hand portions of each map. Measurements taken in the vertical dipole orientation were more susceptible to the *cultural noise* interference caused by these fence lines. The multiple *humps* along the lower portion of the maps are caused by this interference. The graphic forms of these humps are products of the interference and the plotting routine.

In the maps of Figure 2, a berm area has been identified. The berm is slightly higher lying than the adjoining areas within the grid. It is characterized and defined by slightly lower values of apparent conductivity. The lower conductivity of the berm materials is attributed to the suspected deposit of more coarser-textured alluvial materials that had been dredged from an adjoining stream channel to construct a nearby pond. The spatial patterns of apparent conductivity shown in Figure 2 fail to indicate the presence of buried structural remnants of the Old Ponca Agency building.

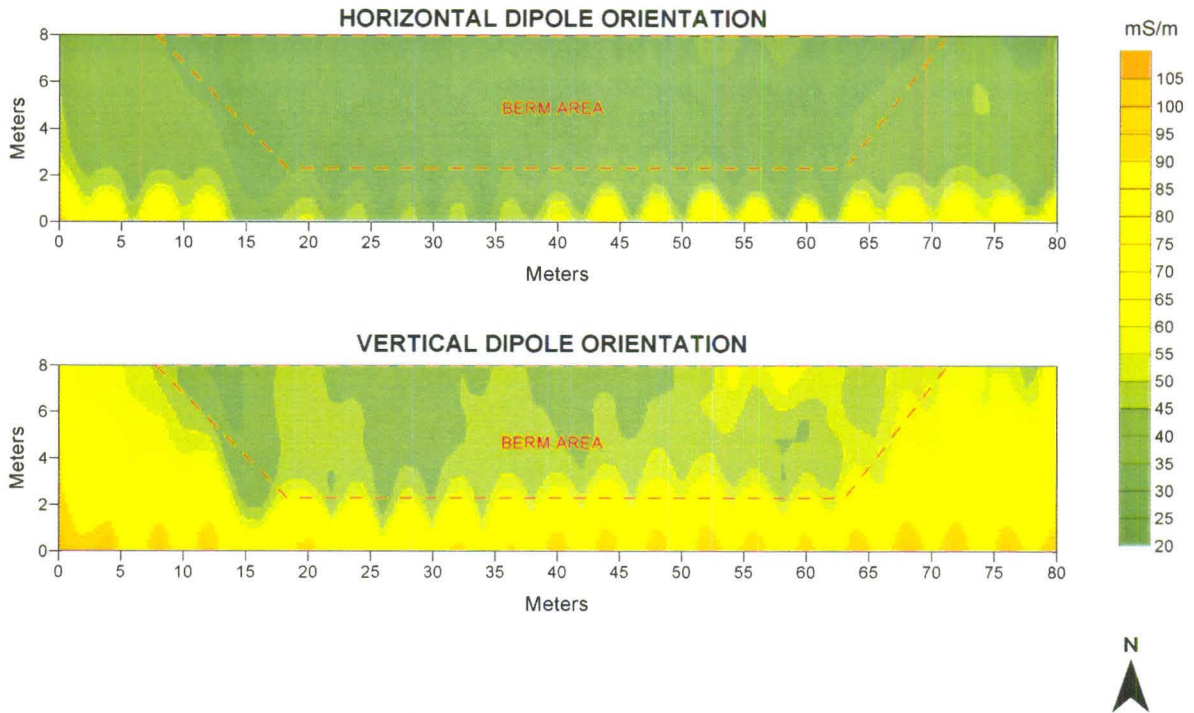


Figure 2. EMI maps of the suspected Old Agency building site and the berm area.

St. Johns Cemetery sites:

Figure 3 contains choropleth maps showing the spatial distribution of apparent conductivity collected with the EM38DD meter at Site 1 within St. Johns Cemetery. These maps have been constructed from 178 observations. Color variations have been used to show the distribution of apparent conductivity. In each map, the color interval is 2 mS/m. In general, EMI responses were slightly higher and more variable in the deeper-sensing, vertical dipole orientation (right-hand map) than in the shallower-sensing, horizontal dipole orientation (left-hand map). Spatial patterns evident in the maps are principally attributed to lateral and vertical variations in clay and carbonate contents. The spatial patterns shown in the maps appear to correspond with known soil patterns. Areas of Labu and Sansarc soils occupy the lower-lying eastern portion of the grid area. Surface layers became lighter textured towards the higher-lying western portion of the grid area. Soils in this portion of the grid are believed to be Simeon or similar soils. The patterns shown in Figure 3 suggest the transition from fine-textured Labu and Sansarc soils on lower-lying backslope positions to coarse-textured Simeon soils on the higher-lying crest of a knoll. There is no clear and unmistakable evidence suggesting disturbance or possible gravesites in these EMI maps. However, while most patterns are broad, linear, and conform to a known transition in soils, several weakly-expressed, low apparent conductivity *spots* are evident in the extreme southwest corner of the grid area. While no cause for these *spot* anomalies is possible at this time without ground-truth verification, they do occur near a clump of trees that contains several marked gravesites.

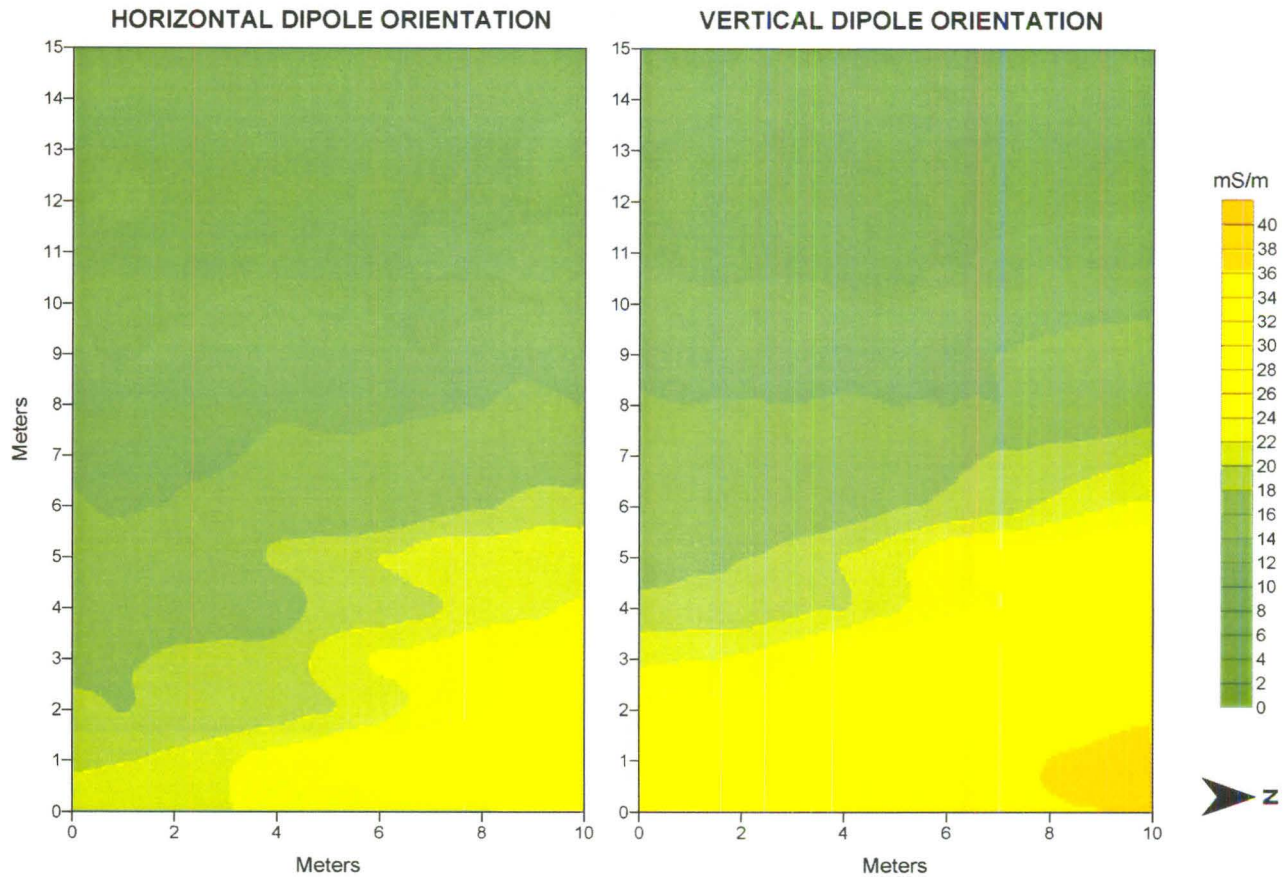


Figure 3. EMI maps of Site 1 within St Johns Cemetery.

Basic statistics for the data collected with the EM38DD meter at Site 1 within St. Johns Cemetery are shown in Table 2. Apparent conductivity increased slightly and became more variable with increasing penetration depths. Apparent conductivity averaged 15.8 mS/m and 18.5 mS/m for measurements obtained in the shallower-sensing horizontal and deeper sensing vertical dipole orientations, respectively. In the horizontal dipole orientation, apparent conductivity ranged from about 9.9 to 27.9 mS/m with a standard deviation of 4.7 mS/m. In the vertical dipole orientation, apparent conductivity ranged from about 9.4 to 40 mS/m with a standard deviation of 8.1 mS/m. The relatively low apparent conductivity at this site was attributed to the large area of coarse-textured Simeon soil.

Table 2
Apparent conductivity data collected with the EM38DD meter at Site 1, St. Johns Cemetery
 All values are in mS/m.

	<u>Horizontal Dipole</u>	<u>Vertical Dipole</u>
Average	15.8	18.5
Standard Deviation	4.7	8.1
Minimum	9.9	9.4
Maximum	27.9	40.0
25% Quartile	11.7	11.7
75% Quartile	19.2	24.7

Figure 4 contains choropleth maps showing the spatial distribution of apparent conductivity collected with the EM38DD meter at Site 2 within St. Johns Cemetery. These maps have been constructed from 196 observations. Color variations have been used to show the distribution of apparent conductivity. In each map the color interval is 2 mS/m. Once again, EMI responses were generally higher and more variable for measurements obtained in the deeper-sensing, vertical dipole orientation (right-hand map) than in the shallower-sensing, horizontal dipole orientation (left-hand map).

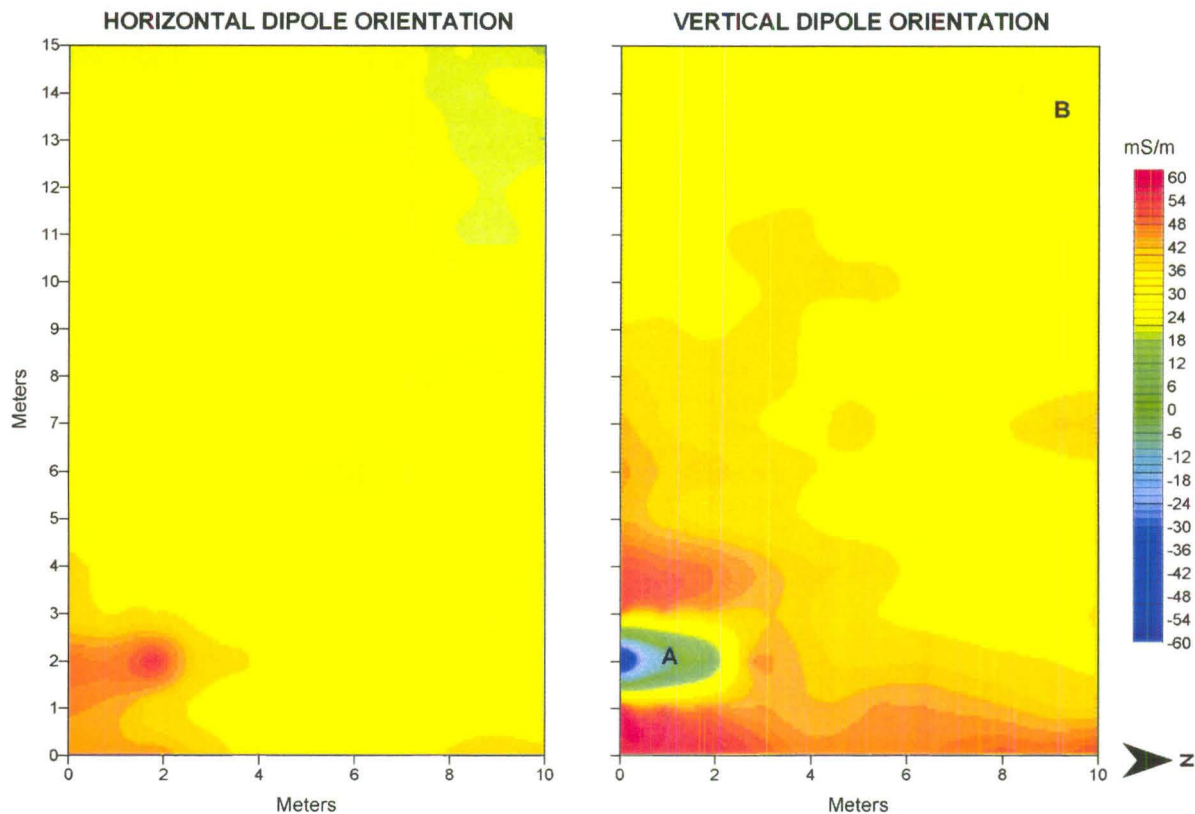


Figure 4. EMI maps of Site 2 within St Johns Cemetery.

Spatial patterns evident in these maps (Figure 4) are attributed principally to lateral and vertical variations in clay and carbonate contents. Within this site, soils are believed to dominantly Labu. Higher apparent conductivity values at this site correspond to the pervasiveness of the high clay content Labu soil. The highest elevation is located in the northwest corner of the grid. The lowest elevation is in the southeast corner of the grid. Lower values in the northwest corner may reflect a mantle of coarser textured soil materials.

In Figure 4, a buried metallic object was crossed at *A*, and a faint anomaly appears near *B*. In the vertical dipole orientation map, the buried metallic anomaly is identified by a phase reversal (negative value flanked by higher positive apparent conductivity). As this feature was barely detected in the horizontal dipole orientation (0 to 0.75 m), we can infer its depth. As this feature occurs in the lowest part of the grid site, a buried drained may be responsible for this response. While several *spot* anomalies occur throughout the grid area, the weakly expressed *spot* anomaly near *B* is intriguing as it is in close proximity to three headstones located to the immediate northwest of the grid area.

Basic statistics for the data collected with the EM38DD meter at Site 2 within St. Johns Cemetery are shown in Table 3. Apparent conductivity increased slightly and became more variable with increasing observation depths. Apparent conductivity averaged 27.8 mS/m and 34.8 mS/m for measurements obtained in the shallower-sensing horizontal and deeper sensing vertical dipole orientations, respectively. In the horizontal dipole orientation, apparent conductivity ranged from about 18.4 to 54.8 mS/m with a standard deviation of 5.5 mS/m. In the vertical dipole orientation, apparent

conductivity ranged from about -55.9 to 58.1 mS/m with a standard deviation of 10.3 mS/m. Compared with Site 1, the higher apparent conductivity at this site was attributed to a greater proportion of fine-textured, more conductive soils within the grid area. Negative values were attributed to the buried metallic object.

Table 3
Apparent conductivity data collected with the EM38DD meter at Site 2, St. Johns Cemetery
All values are in mS/m.

	<u>Horizontal Dipole</u>	<u>Vertical Dipole</u>
Average	27.8	34.8
Standard Deviation	5.5	10.3
Minimum	18.4	-55.9
Maximum	54.8	58.1
25% Quartile	24.2	31.2
75% Quartile	29.8	39.5

Santee Sioux Nation Cemetery site:

Basic statistics for the data collected with the EM38DD meter at the suspected Santee Sioux Nation Cemetery are shown in Table 4. Apparent conductivity increased and became slightly more variable with increasing penetration depths. Apparent conductivity averaged 34.8 mS/m and 48.1 mS/m for measurements obtained in the shallower-sensing horizontal and deeper sensing vertical dipole orientations, respectively. In the horizontal dipole orientation, apparent conductivity ranged from about 11.3 to 63.7 mS/m with a standard deviation of 7.8 mS/m. In the vertical dipole orientation, apparent conductivity ranged from about 26.2 to 85.1 mS/m with a standard deviation of 9.3 mS/m.

Table 4
Apparent conductivity data collected with the EM38DD meter at suspected Cemetery Site near Santee
All values are in mS/m.

	<u>Horizontal Dipole</u>	<u>Vertical Dipole</u>
Average	34.8	48.1
Standard Deviation	7.8	9.3
Minimum	11.3	26.2
Maximum	63.7	85.1
25% Quartile	28.9	41.4
75% Quartile	40.0	54.3

Figure 5 contains choropleth maps showing the spatial distribution of apparent conductivity collected with the EM38DD meter at the suspected cemetery site near Santee. These maps have been constructed from 1849 observations. Color variations have been used to show the distribution of apparent conductivity. In each map, the color interval is 2 mS/m. Once again, EMI responses were higher and more variable for measurements obtained in the deeper-sensing, vertical dipole orientation (lower map) than in the shallower-sensing, horizontal dipole orientation (upper map). In each map, the symbol *A* represents the approximate location of a stone marker and iron cross.

In Figure 5, spatial patterns are noticeably elongated in a north-to-south direction across each map (though more prominent in the vertical dipole data). This direction corresponds with the surveying paths. These patterns are artificial. Slight spatial discrepancies will exist in EMI data because of instrument drift, the distance between the transmitting and receiving coils, and the time delay in data logging. These offsets and delays, as well as the surveying methods, are responsible for the elongated *herringbone* patterns that occur in these maps. The larger size of this grid, the inclusion of more sloping areas (affect on walking speeds in upslope and downslope directions), and the reduced positional accuracy contributed to these rather distinct *herringbone* patterns.

A majority of the spatial patterns shown in Figure 5 are believed to represent changes in soil type and properties. Lower values in the central portion of these maps correspond with the crest of a higher-lying, convex knoll. Based on observations made in other portion of Knox County, it is presumed that coarser-textured and less conductive soil materials mantle this landscape position. While more irregular and scattered *spot* patterns are evident in these maps than in other maps shown in this report, the sources of this variability remains unknown. It is easy and tantalizing to conclude that some of these features represent gravesites. Some may be. However, without some ground-truth verification, there is no conclusive or unmistakable evidence that these patterns do represent gravesites.

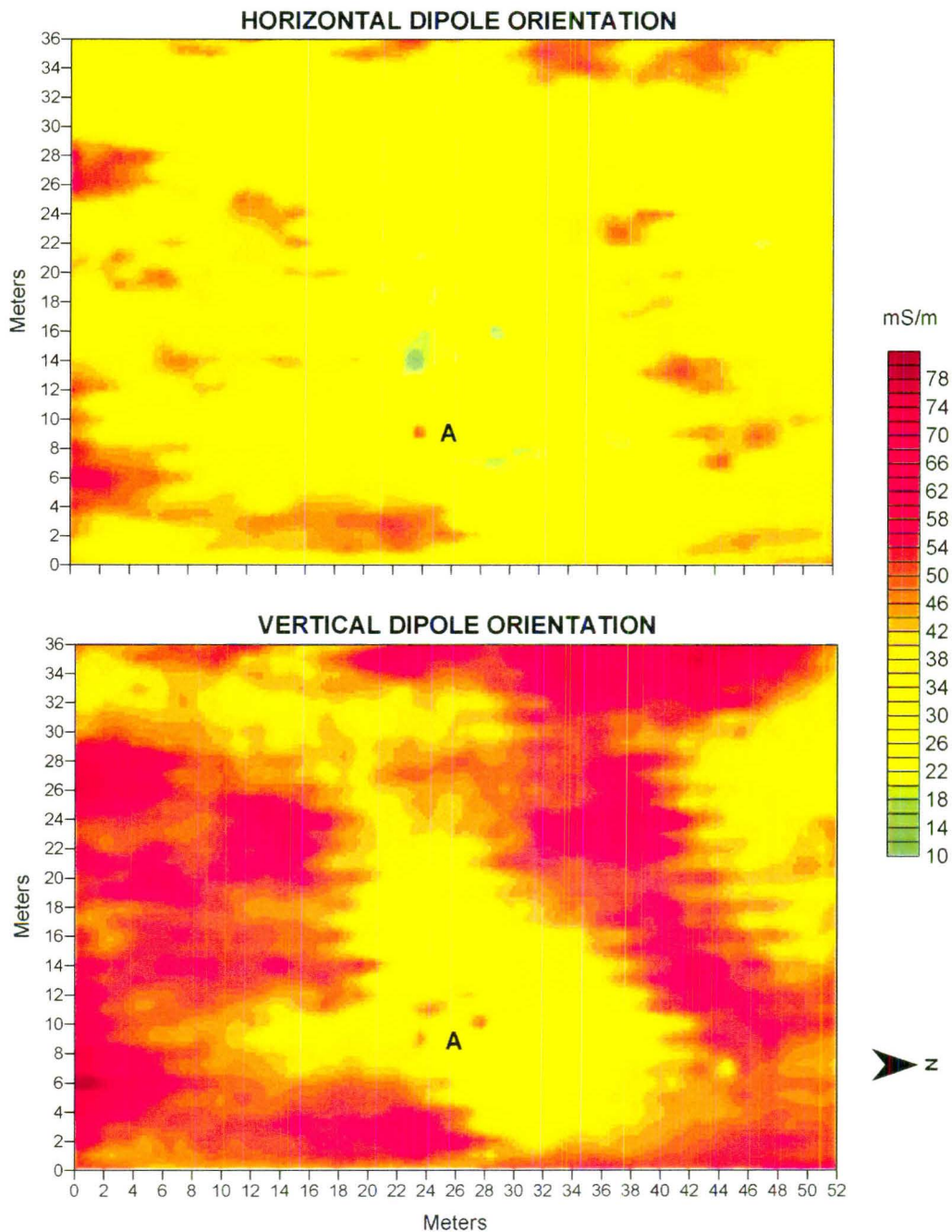


Figure 5. EMI maps of suspected cemetery site near Santee.

GPR:

In general, unfavorable soil properties limited the effectiveness of GPR. The high clay content, large proportion of 2:1 expanding lattice clay minerals with high cation exchange capacities, and high carbonate contents of these soils produced highly conductive mediums. These mediums rapidly attenuate the radar signal and limit the depth of penetration and the detection of subsurface features. Because of high rates of signal attenuation, high levels of background noise plagued radar records and confounded interpretations. Background noise most commonly took the form of low amplitude, diffuse, and parallel reflectors.

Figure 6 is a radar record from the St Johns Cemetery near Ponca. A depth scale (in meters) is located along the left-hand side of the radar profile. The estimated depth scale was based on the depth to a known reflector. For the upper part of the soil profile, the velocity of propagation was assumed to be 0.074 m/ns and the dielectric permittivity was 16 (based on a calibration trial conducted in an area of Verdel soil at the Old Agency site).

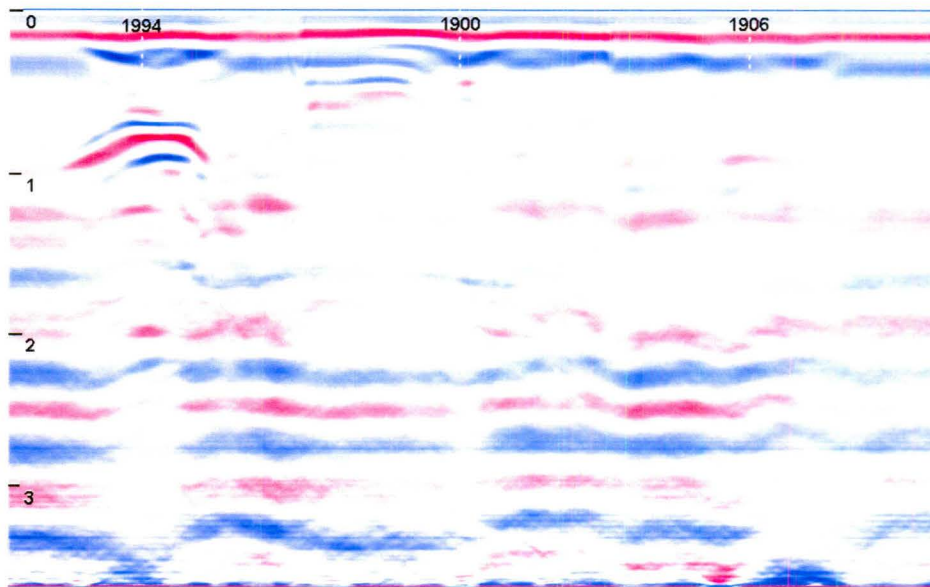


Figure 6. GPR record of three known gravesites in an area of Verdel silty clay, 2 to 6 percent slopes.

The radar record shown in Figure 6 was obtained in an area of Verdel silty clay, 2 to 6 percent slopes (Schulte et al., 1997), located immediately upslope from the cemetery entrance. In this record, three marked graves were traversed with the 400 MHz antenna. The burial dates on the headstones are 1994, 1900, and 1906. Radar traverses were conducted at a 90-degree angle to each headstone and in the middle of the grave. The segmented vertical lines at the top of the radar record mark the middle of each gravesite. Indications of a gravesite are only distinguishable on the most recent gravesite. Here a low mound of earthen materials covers the grave. If subsurface reflections are discernible only on the most recent of three known graves, what are the prospects that GPR will detect old, unmarked graves?

In the radar record shown in Figure 6, the depth of penetration is less than 1 m. Below this depth, broad parallel bands of noise plague the radar record. Severely restricted penetration depths, unobserved subsurface features, and poor interpretative quality made two-dimensional radar records ineffective for burial detection in the investigated soils.

3-D Time sliced image

Three-dimensional interpretations of GPR data have been used to identify burials, middens, and other cultural features (Conyers and Goodman, 1997, Whiting et. al, 2000). This technique is frequently used when buried features are difficult to distinguish or subsurface patterns are chaotic and unrecognizable. Three-dimensional images permit the recognition and mapping of amplitude anomalies that are difficult to distinguish in individual radar records. Based on the processing of sequential two-dimensional radar records within a grid, a 3-D image is generated. With 3-D images, the location,

orientation, and spatial distribution of higher and lower amplitudes at specific depths can be assessed and the subsurface reconstructed.

To construct three-dimensional displays, the imagery between adjoining radar profiles is interpolated. As a consequence, the quality and detail of a three-dimensional display will increase as the spacing between survey lines is decreased (Geophysical Survey Systems, Inc., 2001b). As a general rule, lines should be spaced so that the radar beams from adjacent lines overlap at the depth of interest (Geophysical Survey Systems, Inc., 2001b). Generally these lines should be closely spaced (0.5 to 1 m apart). In this study lines were spaced 1 m apart.

3-D time-sliced images were prepared from GPR data recorded within each grid area. “Slices” were made across each cube at arbitrary depths. The depth scales used in the 3-D images are based on a propagation velocity of 0.07 m/ns. This scale assumes that the velocity of propagation remains constant with increasing depth through the soils. As this is not true, time-slices are considered only approximations of actual depth slices. At each site, the ground surface was uneven and sloping. As the radar data were not topographically corrected, though each slice is parallel to the surface, departures from a true horizontal plane occur.

Signal processing is used in the preparation of 3-D images to remove or minimize background noise and clutter in the data. As noted by Daniels and others (1997), while processing tends to improve the appearance of the data, it rarely changes interpretations. Simplifying the radar profile through the elimination of noise and clutter is a prerequisite for achieving favorable interpretations (Daniels et al., 1997). In addition to range gain and color table and transformation adjustments, all radar records were migrated to reduce hyperbolic diffraction patterns.

Interpretations of 3-D images are biased towards high amplitude in-line reflectors. Maximum amplitude processing eliminates all data other than peak values (Daniels et al. 1997). This reduces background noise and improves the clarity of the 3-D image. Reflectors that are out of line from the original radar traverse are minimized in 3-D images because they are not align horizontally and do not add constructively in the horizontal direction (Daniels et al., 1997).

Features with complicated shapes and subsurface topographies produce complex scattering of electromagnetic energy that results in awkward and difficult to interpret 3-D images. Decreasing the thickness of the time slice (finite-width slice) was used to improve the visual presentation and interpretations by isolating and defining features in greater detail.

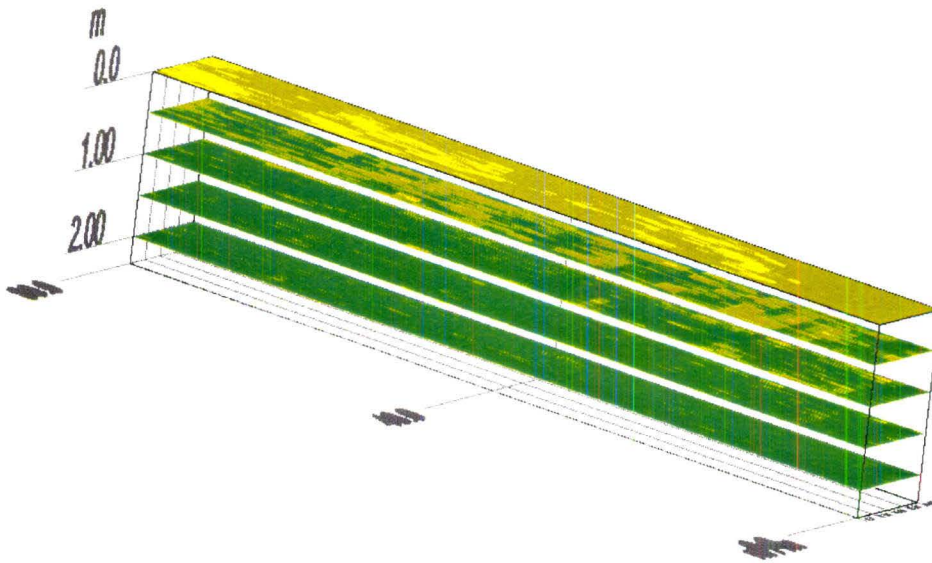


Figure 7. 3-D time-sliced images from composite radar records obtained at the Ponca Agency Site. All units of measurement are in meters. Origin is located in the northwest corner of the grid.

Figure 7 shows four time-sliced or *plane view* images of the Ponca Agency site. Slices have been made at depths of 0, 50,

100, 150, and 200 cm. Figure 7 is admittedly very small and difficult to view. However, no repeating linear or rectangular patterns with dimensions suggesting a building site are evident in the time-sliced images. Patterns evident in the surface layers (0.0 and 0.5 m slices) reflect soil interfaces. If present, remnants from the former Ponca Agency are too small or lack sufficient contrast to be detected with GPR.

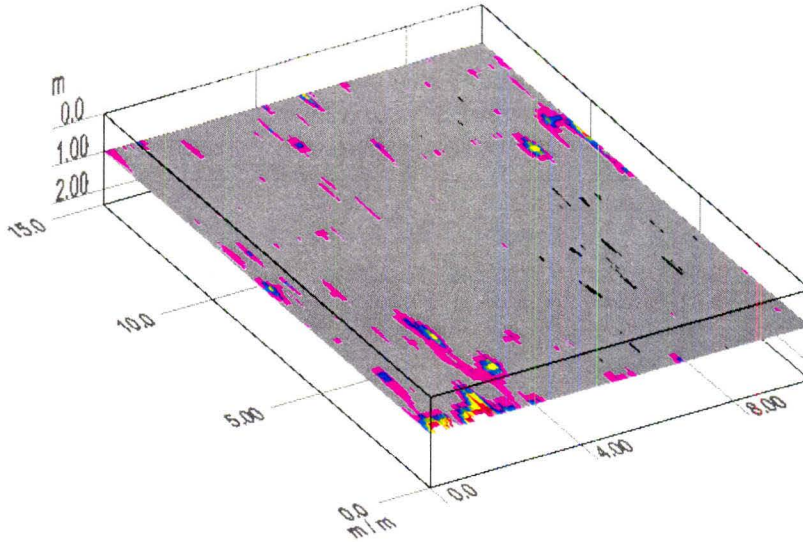


Figure 8. A 3-D time-sliced image of composite radar records obtained at Site 1, St. John Cemetery. Time slice is at 1 meter. All units of measurement are in meters. Origin is located in the southeast corner of the grid.

Figure 8 shows a time-sliced image of Site 1 within St Johns Cemetery. The slice has been made at depths of about 1 m. Several repeating linear or rectangular patterns with dimensions suggesting gravesites are evident in this time-sliced image. The most prominent reflectors are located in the southeast (lower left-hand) and northwest (upper right-hand) corners of the survey area. The more extensive patterns of high amplitude reflectors in the southeast corner may reflect soil interfaces. A few point reflectors are evident in the southwest (upper left-hand) corner of the grid. This is the portion of the grid area that contained the *spots* recorded with the EM38DD meter (see Figure 3). Though several subsurface reflectors that suggest burials are evident in this image, without some form of ground truth verification, no one feature can be unmistakably identified as a burial.

Figure 9 shows a time-sliced image of Site 2 within St Johns Cemetery. The slice has been made at a depth of about 90 cm. Compared with Site 1, Site 2 contains few high amplitude, repeating linear patterns with dimensions suggestive of gravesites. A fairly conspicuous linear reflector is located in the northeast (lower right-hand) corner of the survey area. Because of its higher amplitude and east-west orientation, this feature offers the most favorable pattern that suggests a possible gravesite. A more restricted high amplitude reflection (near lower left-hand corner) occurs in the general vicinity of the buried metallic anomaly detected with EMI (see Figure 4). Though several weakly expressed subsurface reflectors suggest possible gravesites, patterns are too weak and ambiguous to be identified as burials.

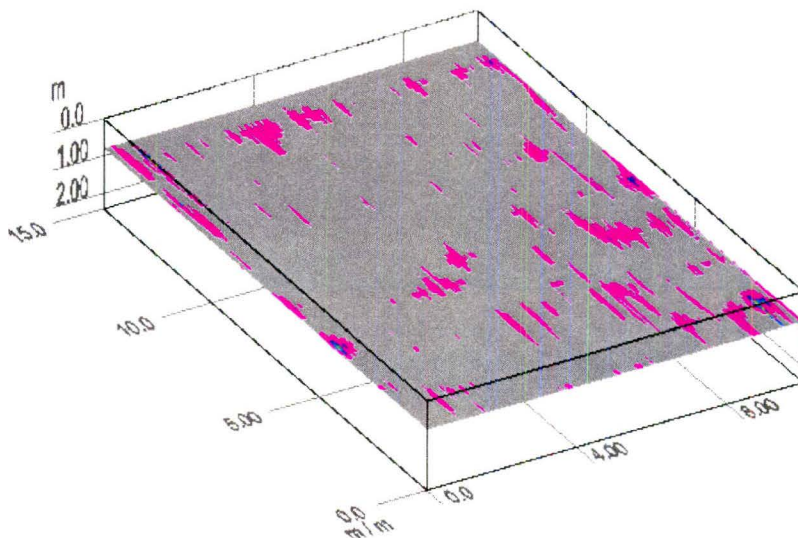


Figure 9. A 3-D time-sliced image of composite radar records obtained at Site 2, St. John Cemetery. Time slice is at 0.9 meter. All units of measurement are in meters. Origin is located in the southeast corner of the grid.

Figure 10 shows a time-sliced image of the southern half of the suspected cemetery site near Santee. The origin of the grid is located in the northeast corner (of the subset grid) and on the western end of line 26 of the main grid (see Figure 5). The slice has been made at a depth of about 100 cm. Very few high amplitude reflections are apparent in this image. Most are too small to suggest a gravesite. However, as confirmed in the radar record shown in Figure 6, in these soils, burials provide few large, lasting, and unambiguous reflectors to GPR. Often, reflectors from a burial are small, faintly expressed, and indistinguishable from other features in the soil (burrows, roots, rock fragments). Several weakly expressed subsurface reflectors are apparent in the western portion (lower foreground) of the grid area shown in Figure 10. All are too small, weakly expressed, and ambiguous to be identified as burials.

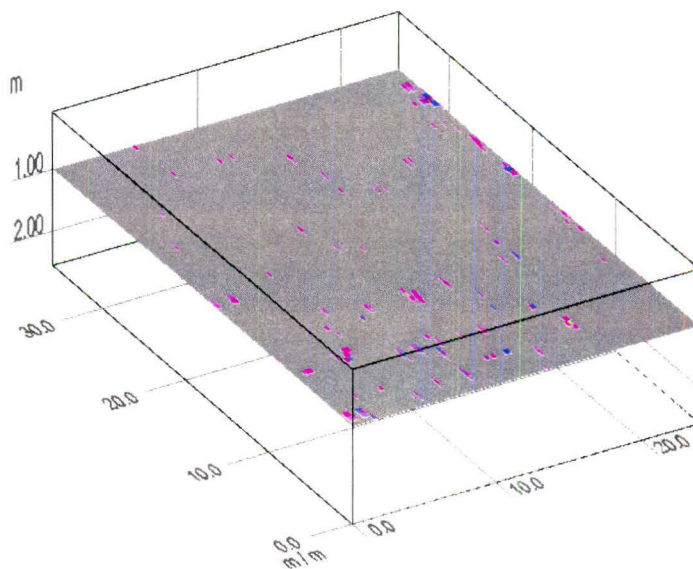


Figure 10. A 3-D time-sliced image of composite radar records obtained at the southern portion of the suspected cemetery site near Santee. Time slice is at 1 meter. All units of measurement are in meters. Origin is located in the northwest corner of the grid.

Figure 11 shows a time-sliced image of the northern half of the suspected cemetery site near Santee. The origin of the grid is located in the northeast corner (of the subset grid) and on the western end of line 52 of the main grid (see Figure 5). The slice has been made at a depth of about 100 cm. Spatial patterns evident in northern portion of the main grid are similar to those seen in the southern subset grid. Similar to the pattern shown in Figure 10, most reflectors in Figure 11 are too small and ambiguous to unequivocally suggest a gravesite. Once again, most subsurface reflectors occur in the western portion of the survey area. Compared with the pattern shown in Figure 10, these reflectors are generally more numerous, larger, and more strongly expressed. Based on radar imagery, the western portion of the main grid provides the most promising area for additional gravesites.

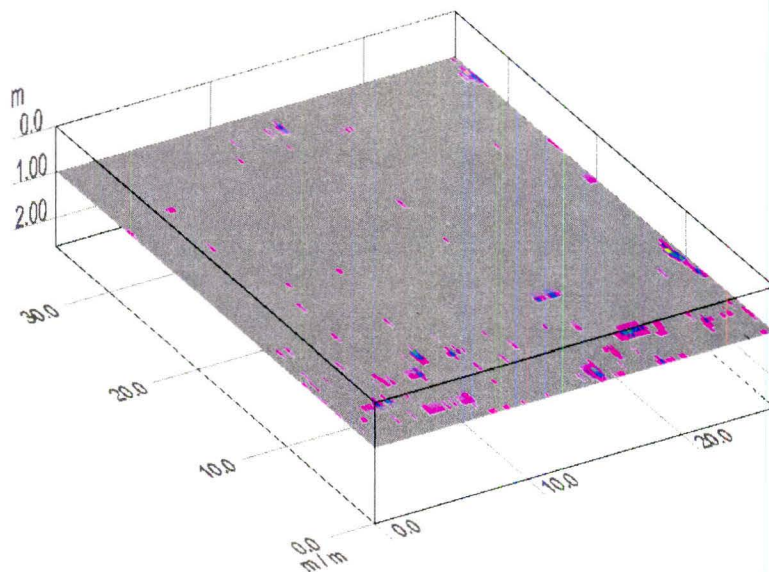


Figure 11. A 3-D time-sliced image of composite radar records obtained at the northern portion of the suspected cemetery site near Santee. Time slice is at 1 meter. All units of measurement are in meters. Origin is located in the northwest corner of the grid.

References:

Bevan, B. W. 1991. The search for graves. *Geophysics* 56(9):1310-1319.

Conyers, L. B., and D. Goodman. 1997. *Ground-penetrating Radar; an introduction for archaeologists*. AltaMira Press, Walnut Creek, CA.

Daniels, D. J. 1996. *Surface-Penetrating Radar*. The Institute of Electrical Engineers, London, United Kingdom.

Daniels, J. J., D. L. Grumman, and M. Vendl. 1997. Coincident antenna three dimensional GPR. *Journal of Environmental and Engineering Geophysics* 2(1): 1-9.

Doolittle, J. A. 1987. Using ground-penetrating radar to increase the quality and efficiency of soil surveys. 11-32 pp. IN: Reybold, W. U. and G. W. Peterson (eds.) *Soil Survey Techniques*, Soil Science Society of America. Special Publication No. 20.

Geonics Limited. 2000. EM38DD ground conductivity meter: Dual dipole version operating manual. Geonics Ltd., Mississauga, Ontario.

Geophysical Survey Systems, Inc, 2001a. RADAN for Windows NT; User's Manual - Condensed. Manual MN43-132 Rev C. Geophysical Survey Systems, Inc., North Salem, New Hampshire.

Geophysical Survey Systems, Inc, 2001b. 3-D QuickDraw for RADAN NT; User's Manual. Manual MN43-143 Rev B. Geophysical Survey Systems, Inc., North Salem, New Hampshire.

Killam, E. W. 1990. The detection of human remains. Charles C. Thomas Publisher, Springfield, Illinois. p. 263

Morey, R. M. 1974. Continuous subsurface profiling by impulse radar. 212-232 pp. IN: Proceedings, ASCE Engineering Foundation Conference on Subsurface Exploration for Underground Excavations and Heavy Construction, held at Henniker, New Hampshire. Aug. 11-16, 1974.

Olhoeft, G. R. 1986. Electrical properties from 10^{-3} to 10^9 Hz – Physics and chemistry. 281-298 pp. IN: Bananvar, J. R., J. Koplik, and K. W. Winkler (Ed.) Proceeding of 2nd International Symp. Physics and Chemistry of Porous Media. Schlumberger-Doll, Ridgefield, Connecticut. October 1986. Am. Inst. Phys., New York, New York, Conference Proceedings.

Schulte, R. B., M. E. Willoughby, J. Carlson, and C. F. Mahnke. 1997. Soil Survey of Knox County, Nebraska. USDA-NRCS and the University of Nebraska, Conservation and Survey Division. U. S. Government Printing Office, Washington DC.

Sternberg, B. K., and J. W. McGill. 1995. Archaeology studies in southern Arizona using ground penetrating radar. Journal of Applied Geophysics 33: 209-225.

Vickers, R., L. Dolphin, and D. Johnson. 1976. Archaeological investigations at Chaco Canyon using subsurface radar. pp. 81-101. In: Remote Sensing Experiments in Cultural Resource Studies, assembled by Thomas R. Lyons, Chaco Center, USDI-NPS and University of New Mexico.

Whiting, B. M. D., McFarland, D. P., S. Hackenberger. 2000. Preliminary results of three-dimensional GPR-based study of a prehistoric site in Barbados, West Indies. 260-267 pp. IN: (Noon, D. ed.) Proceedings Eight International Conference on Ground-Penetrating Radar. May 23 to 26, 2000, Goldcoast, Queensland, Australia. The University of Queensland.